Available online at www.sciencedirect.com
ScienceDirect
Journal of Photochemistry and Photobiology A: Chemistry 183 (2006) 238–246
Journal of Photochemistry and Photobiology A:Chemistry
www.elsevier.com/locate/jphotochem

Fluorescence of molecular micro- and nanocrystals prepared with Bodipy derivatives

Sophie Badré [a], Virginie Monnier [b], Rachel Méallet-Renault [a,*], Cécile Dumas-Verdes [a], Elena Yu. Schmidt [c], Al'bina I. Mikhaleva [c], Guillaume Laurent [d], Georges Levi [d], Alain Ibanez [b], Boris A. Trofimov [c], Robert B. Pansu [a]

[a] *Laboratoire de Photophysique et Photochimie Supramoléculaires et Macromoléculaires, CNRS UMR 8531, Ecole Normale Supérieure de Cachan, 61 Avenue de Président Wilson, 94235 Cachan Cedex, France*
[b] *Laboratoire de Cristallographie, CNRS UPR 5031, Université Joseph Fourier and Institut National Polytechnique de Grenoble, BP 166, 38042 Grenoble Cedex 09, France*
[c] *A.E. Favorsky Irkutsk Institute of Chemistry, Siberian Branch of the Russian Academy of Sciences, Irkutsk 664033, Russian Federation*
[d] *ITODYS, CNRS UMR7086 U. Denis Diderot Paris VII, 1 Rue Guy de la Brosse, 75005 Paris, France*

Available online 11 July 2006

Abstract

Trimesitylbodipy (TMB), a new 4,4-difluoro-4-bora-3a,4a-diaza-*s*-indacene derivative with bulky side groups, was synthesized in order to develop nanostructured fluorescent devices. Fluorescence properties of TMB were studied in dichloromethane, in amorphous films prepared by rapid evaporation of a solution and in micro- and nanocrystals. It was compared to the spectroscopy of Mesitylbodipy (MB) to see if the mesityl groups of TMB modify fluorescence in the solid state. A set-up including a space and time correlated photon-counting photo-multiplier was used to record fluorescence intensity and lifetime images of solids. For both dyes, the formation of fluorescent excimers was observed. There is evidence to suggest energy transfer from monomer to both fluorescent and non-fluorescent excimers. MB fluorescence is still quenched in the crystalline state but in TMB monocrystals the fluorescence comes from only one excimer with a lifetime of 9.5 ns. TMB nanocrystals with a monoexponential fluorescence decay were also prepared.

Keywords: Bodipy; Organic nanocrystals; Fluorescence

1. Introduction

Single fluorescent molecules are widely used to design highly sensitive sensors [1,2]. Fluorescence allows the detection of single fluorophores [3,4] but assemblies of fluorescent molecules in micro- or nano-particles can provide even more responsive sensors due to their high absorption cross-section and their capability of quenching more than one fluorophore per sensor [5–7]. Unfortunately, fluorescent molecules in such dense assemblies have a tendency to form non-fluorescent excitons [8]. Many strategies have been used to build fluorescent assemblies where strong interactions between neighbours, that are responsible for the loss of fluorescence, are prevented: doped zeolites [9], rigid dendrimers [10,11] doped latex [7,12], and polymers [13]. Even more dense packing of molecules can be observed in crystals. Fluorescent molecular crystals can be prepared by reprecipitation in water or in sol–gel matrix [14–17].

In this context, we have chosen to design new organic molecules that could exhibit fluorescence in the solid state. We have selected dyes of the Bodipy family i.e. 4,4-difluoro-4-bora-3a,4a-diaza-*s*-indacene derivatives. Bodipy derivatives have many applications: they are used as laser dyes [18,19], biological markers [20] and in sensing devices [21–23], some of which are patented [24]. They are photostable dyes and their fluorescence quantum yield is generally high (above 0.5). Fluorescent crystals of Bodipy might find many applications since the pigments (solid dyes) based on them should show high brightness and enhanced resistance to photobleaching. We want to develop fluorophores where the Bodipy core is isolated from its neighbours in the solid state by bulky mesityl substituents [25,26]. Then π-stacking would be prevented at high concen-

Abbreviations: TMB, trimesitylbodipy; MB, mesitylbodipy

* Corresponding author. Tel.: +33 1 47 40 76 61; fax: +33 1 47 40 24 54.
E-mail address: rachel.meallet@ppsm.ens-cachan.fr (R. Méallet-Renault).

1010-6030/$ – see front matter © 2006 Elsevier B.V. All rights reserved.
doi:10.1016/j.jphotochem.2006.07.002

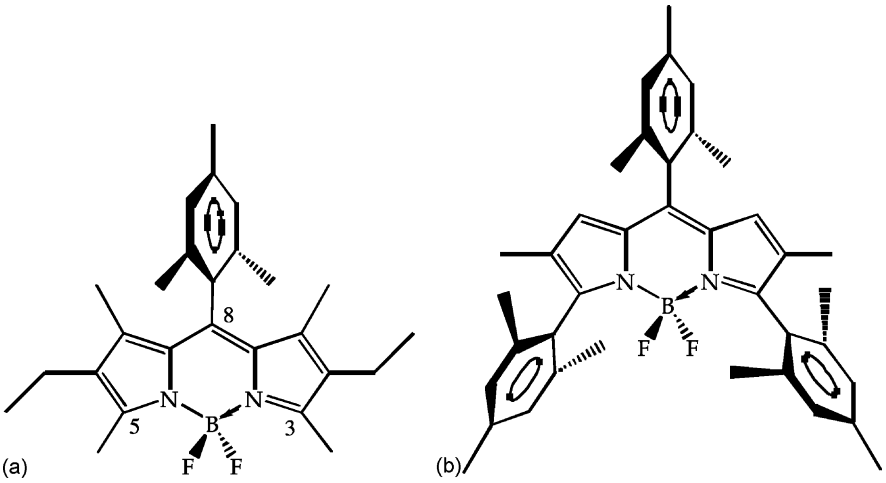

Fig. 1. Molecular structure of: (a) mesitylbodipy and (b) trimesitylbodipy.

trations. Indeed this kind of interaction is considered to be the principal culprit behind the loss of fluorescence in crystalline form.

In this paper, we report the synthesis, which was described in detail previously [27], and the spectroscopic properties of a new fluorescent dye, the Tri-Mesityl-Bodipy (TMB) The dye was studied in different environments: dissolved in dichloromethane, in amorphous films prepared by rapid evaporation of a solution, in macrocrystals and nanocrystals grown in the pores of sol–gel matrices. Fluorescence imaging is used to study the various samples. We also compare TMB properties with those of a previous dye we have designed (Mesityl-Bodipy referred to as MB [7]) in order to determine the effect of the mesityl groups added to the Bodipy core (see Fig. 1).

2. Experimental

2.1. Chemicals

All chemicals were used as purchased. All solvents were of spectroscopic grade, except for TMB synthesis where anhydrous dichloromethane was used.

2.2. Synthesis of trimesitylbodipy and mesitylbodipy

The synthesis of TMB and MB have been described elsewhere [28,7]. The mesitylpyrrole was synthesized at the Irkutsk Institute of Chemistry using the Trofimov reaction [27]. The following procedure was used for both dyes [28]: a solution of the pyrrole in dried CH_2Cl_2 was condensed at room temperature with 2,4,6-trimethylbenzaldehyde under acid catalysis to get the corresponding dipyrromethane. Oxidation by DDQ (2,3-dichloro-5,6-dicyanobenzoquinone) gives the dipyromethene moiety. Bodipy was obtained by adding boron trifluoride etherate along with diisopropylethylamine. TMB was then purified using flash-chromatography on silica (CH_2Cl_2/petroleum ether 1:3 volume ratio as eluent). After solvent evaporation a violet solid was obtained. The global reaction yield was 45%. MB was purified by chromatography on a neutral alumina column (CH_2Cl_2/petroleum ether, 1:1). The overall yield of this synthesis was 70%.

2.3. Free microcrystals and cast films

Fluorescence properties of TMB and MB in dense assemblies were first studied on cast films prepared by evaporation of a droplet of the dye solution in dichloromethane spread out on microscope slides. Microcrystals grown right after the synthesis were also studied.

2.4. Raman spectroscopy

In order to estimate their crystallinity, Raman spectra of microcrystals and casted films were recorded. To do so, an Olympus BH-2 microscope coupled with a DILOR XY microspectrometer was used. The excitation wavelength was set at 647.1 nm. The spectra were recorded between 970 and 1375 cm^{-1} (emission centred at 1200 cm^{-1}, corresponding to 690.5–710.3 nm). The spectra showed were recorded with a laser power of 4 $mW \cdot cm^{-2}$.

2.5. Nanocrystals in sol–gel thin-films

The starting solution was prepared with silicon alkoxides used as sol–gel precursors, tetrahydrofuran (THF), Bodipy powder, and a small amount of water for the hydrolysis of the alkoxides [29]. An equimolar alkoxide mixture of TMOS (tetramethoxysilane) and MTMOS (methyltrimethoxysilane) was used. THF allowed the Bodipy powder to dissolve and mixing of the water with the alkoxides. The [solvent]/[alkoxide] molar ratio was set to 5 for all the thin films studied here. The dye amount, expressed by the molar ratio d = [organic]/[alkoxide], was adjusted to control the particles size. d was ranging in this study between 1×10^{-3} and 1×10^{-2} leading to nanocrystals sizes ranging between 100 and 650 nm in diameter (Table 3). Two samples were prepared with MB (MB1 and MB2) and three with TMB (TMB1 to TMB3). Sols involved in the preparation of samples MB1, MB2, TMB1 and TMB2 were prepared under

acid catalyzed conditions by one-step of hydrolysis and condensation of the TMOS + MTMOS alkoxide precursors. For sample TMB3, a two-step hydrolysis and condensation was applied under acid–base conditions [30,31]. The resulting sols were deposited at room temperature by spin coating onto microscope slides with a rotation speed of 4000 rpm. These nanocomposite coatings were then stabilized by annealing at 100 °C in order to remove any residual solvent and to improve the crystal quality of the particles [32].

The nanocrystals were observed by confocal microscopy or transmission electron microscopy (TEM). The images were analysed using Scion Image for Windows (Scion Corporation), a software based on NIH (National Institute of Health) Image for MacIntosh (http://www.rsb.info.nih.gov/nih-image/), in order to quantify accurately particle size and size distribution. In confocal microscopy the light source was the 488 nm beam of a 15 mW Argon laser and the microscope was a LSM510 from Zeiss. For TEM characterizations, the sols were deposited onto sodium chloride crystal plates. These substrates were dissolved in water in order to image only the sol–gel thin film placed on a copper grid. A Phillips CM300 microscope working at 300 kV was used for this characterization.

2.6. Steady-state and time resolved spectroscopy

UV–vis absorption spectra were measured with a Varian CARY 500 spectrophotometer. Excitation and emission spectra were measured on a SPEX Fluorolog-3 (Jobin-Yvon). The solvent used was dichloromethane. For liquid samples, right-angle configuration was used and optical density was adjusted below 0.1 to avoid reabsorption artefacts. Absorption and fluorescence of films were studied with the SPEX Fluorolog-3 in front face configuration and with an Ocean Optics S2000 miniature fibre optic spectrophotometer under microscope.

Fluorescence decay curves were obtained with the time-correlated single-photon-counting method using a titanium–sapphire laser pumped by an argon ion laser (82 MHz, 1 ps pulse width, repetition rate lowered to 4 MHz thanks to a pulse-picker, a doubling crystal was used to reach 495 nm excitation) [33]. The Levenberg–Marquardt algorithm was used for non-linear least square fit [34]. In order to estimate the goodness of the fit, the weighted residuals were plotted [35]. In the case of single photon counting, they are defined as the residuals, i.e. the difference between the measured value and the fit, divided by the square root of the fit. χ^2 is equal to the variance of the weighted residuals. A fit was said good for χ^2 values below 1.2.

2.7. Intensity and fluorescence lifetime imaging

FLIM and intensity images of solid samples were recorded using a space and time correlated photon-counting photomultiplier (QA) installed on a NIKON TE 2000 microscope. The light source was the titanium–sapphire laser described in Section 2.6. The samples were studied under wide field illumination. For some experiments, a band-pass filter was added at the output of the microscope, in order to narrow the emission wavelength range. The bandwidth of the filter is 6 nm for filters centred at 619 nm and below and 8 nm for filters at 639 nm and more. The QA was purchased from Europhoton Gmbh (Berlin). It is a multi-channel plate photo-multiplier working in the single photon counting mode (Fig. 2). The anode is divided into four quadrants. A fifth conductive part is placed around these four anodes in order to improve the detector precision in points located at the borders of the field. When a photoelectron is produced, an avalanche is created in the two multichannel plates and spread over the five anodes. The position of the photon on the photocathode can be calculated from a weighted mean of the five charges collected. For each photon detected, the delay between the laser pulse and the arrival of the photon on the photomultiplier, the absolute arrival time (i.e. the time from the beginning of the measurement) and the position of the photon on the photocathode are measured and saved on a hard disk. The histogram of the number of photons collected per pixel gives an intensity image of the sample. The histogram of the number of photons collected as a function of absolute arrival time gives the evolution of the global fluorescence intensity and a way to monitor photobleaching. The average fluorescence lifetime τ for each pixel was calculated by dividing the sum of all the delays between the laser pulse and the exact moment that the photon is collected, τ_i, by the number of incident photons on that pixel, N, i.e. $\tau = (1/N)\sum_1^N \tau_i$. It is a fast and robust way to do FLIM. Fluorescence decay curves were constructed as the histogram of the number of photons collected as a function of the fluorescence delay. The collection is done over all the pixels in a specific area. Unless otherwise stated, the fluorescence lifetimes given in this paper correspond to the global fluorescence decay, i.e. the decay corresponding to the whole QA image. The instrument response time is 150 ps (FWHM) and the spatial resolution of our set-up is 300 nm (FWHM).

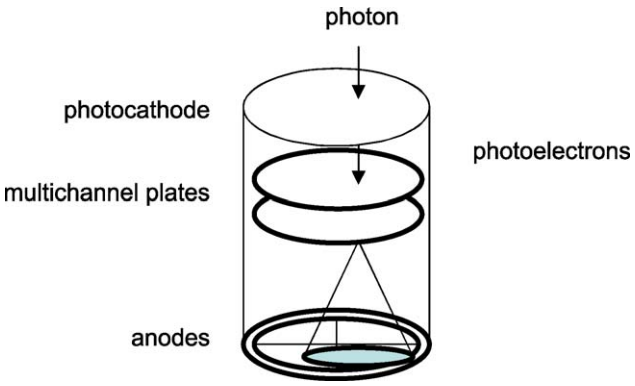

Fig. 2. Schematic view of the space and time correlated photon-counting photomultiplier (QA).

3. Results and discussion

3.1. UV–vis spectroscopy in dichloromethane

Absorption and fluorescence spectra of Mesitylbodipy and Trimesitylbodipy are shown in Fig. 3. The absorption maxima are located at 526 and 543 nm, corresponding to the $S_0 \rightarrow S_1$ transition, and the fluorescence maxima are located at 535 and

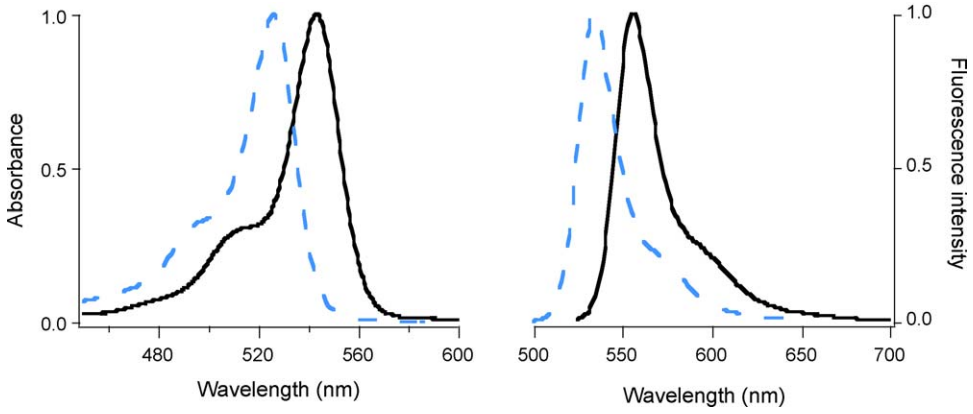

Fig. 3. Absorption (left) and fluorescence (rigth) spectra of MB (dashed line) and TMB (solid line) in dichloromethane.

Table 1
Absorption and fluorescence maxima, molar extinction coefficient, lifetime, quantum yield and hydrodynamic radius of MB and TMB in dichloromethane

	λ_{abs} (nm)	λ_{em} (nm)	ε (cm^{-1} mol^{-1} L)	τ (ns)	ϕ_f
MB	526	535	58000	6.10	0.72
TMB	543	556	80000	6.30	0.90

The χ^2 values are 1.12 for MB and 0.94 for TMB.

556 nm. A second absorption band appears around 350 nm and is attributed to the $S_0 \rightarrow S_2$ transition. The shape of the spectra is typical of Bodipy derivatives. Mesitylbodipy and Trimesitylbodipy have a high molar extinction coefficient (58,000 and 80,000 cm^{-1} mol^{-1} L, respectively, see Table 1) and good quantum yields (0.72 and 0.90). Absorption and fluorescence excitation spectra (data not shown) are in good agreement. The fluorescence lifetimes measured in dichloromethane are 6.10 and 6.30 ns. Both dyes show good photostability as no significant bleaching was observed, even under high power laser irradiation ($I < 200$ mW cm^{-2} for QA experiments). These results agree with those previously obtained for other Bodipy derivatives [20,36]. For example, boron dipyrromethene substituted by 8-(ω-acetoxy) polymethylene chains in different solvents have quantum yields between 0.5 and 0.8 and lifetimes between 4 and 7 ns.

In solution, both MB and TMB have good absorption cross-section and fluorescence quantum yields. A Bodipy similar to MB has already been studied [37]. This molecule has a 4′-iodo-phenyl group at position 8 instead of a mesityl group. The fluorescence properties of this molecule in chloroform are close to those reported for MB. The same article also reports on Bodipys with the same iodo-phenyl group at position 8 and aryl groups at positions 3 and 5 (see Fig. 1). The equivalent of TMB with phenyl groups has a very low quantum yield (0.2 in $CHCl_3$) because of non-radiative relaxation due to the spinning motion of the aryl group around the C-aryl bound. Constraining this relaxation path increases the fluorescence quantum yield [36,38]. In TMB, the mesityl groups are blocked in the plane perpendicular to the plane of the Bodipy core because of the methyl substituents, explaining the high quantum yield observed for this molecule.

3.2. Cast films prepared from dichloromethane solutions and microcrystals

Rapid evaporation of TMB and MB solutions led to the formation of thin films. Fluorescence imaging shows drops a few micrometers wide and a few hundreds of nanometers thick.

Fig. 4 shows the absorption and fluorescence spectra of a TMB cast film as well as the corresponding fluorescence decay. Compared to TMB dissolved in dichloromethane, the absorption spectrum is broader and red-shifted by 10 nm. The fluorescence spectra recorded on different samples have two maxima: one at

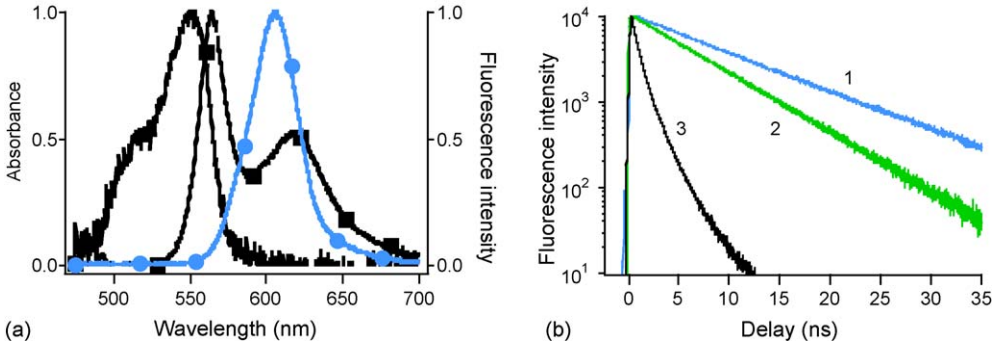

Fig. 4. (a) (—) Absorption spectrum of TMB casted films; (■) fluorescence spectrum of TMB casted films; (●) fluorescence spectrum of a TMB single crystal. In casted films, the broadening of the absorption spectra and the new fluorescence maximum is due to the formation of fluorescent and non-fluorescent excimers. The fluorescent species is an excimer in the crystal. (b) Fluorescence decay of: (1) TMB crystal; (2) TMB in dichloromethane; (3) casted film.

Table 2
First two columns: measured fluorescence maxima and mean lifetimes for solid samples (the value is the average of the values measured on at least five different points ± the standard deviation). Last two columns: central wavelength of the band-pass filters with corresponding mean lifetime for the experiments described in Section 3.2

	λ_{em} (nm)	$<\tau>$	$\lambda_{band\text{-}pass\ filter}$ (nm)	$<\tau>$
MB film	562 ± 3.5	1.36 ± 0.07	No filter	1.30
	635		560	1.07
	739 ± 1		639	1.50
MB powder	608 ± 16	1.28 ± 0.23		
	739 ± 1			
TMB film	569 ± 4	0.5–1.5	No filter	0.54
	619 ± 2.9		560	0.33
			619	0.67
TMB powder	598 ± 12	1.77 ± 0.8		
TMB single crystal	608 ± 3	9.5[a] [1.18]		

[a] Monoexponential decay, the value in parenthesis is the χ^2.

569 ± 4 nm and the second at 619 ± 2.9 nm (Table 2). Depending on the sample, the position of the maxima and the ratio between the two intensities change. The first peak is attributed to fluorescence of TMB monomers while the second one is due to excimers. The fluorescence decays are multiexponential with a mean lifetime between 0.5 and 1.5 ns. For films prepared with MB, the absorption spectrum is broader on the red side compared to the spectrum in dichloromethane. The fluorescence spectra exhibits a broad peak at 562 ± 3.5 nm with, in some cases, a shoulder around 635 nm and a second peak at 739.5 ± 1 nm. The mean fluorescence lifetime is 1.36 ± 0.07 ns (data not shown).

Microcrystalline powders grown during the synthesis were studied (data not shown). Compared to amorphous films, the emission spectra of TMB are broader with one maximum at 598 ± 12 nm. The decay is still multiexponential with a mean lifetime of 1.77 ± 0.8 ns. In the case of MB, two peaks appear: one at 608 ± 16 nm and the other at 739.5 ± 1 nm. The decay is again multiexponential with a mean lifetime of 1.28 ± 0.23 ns.

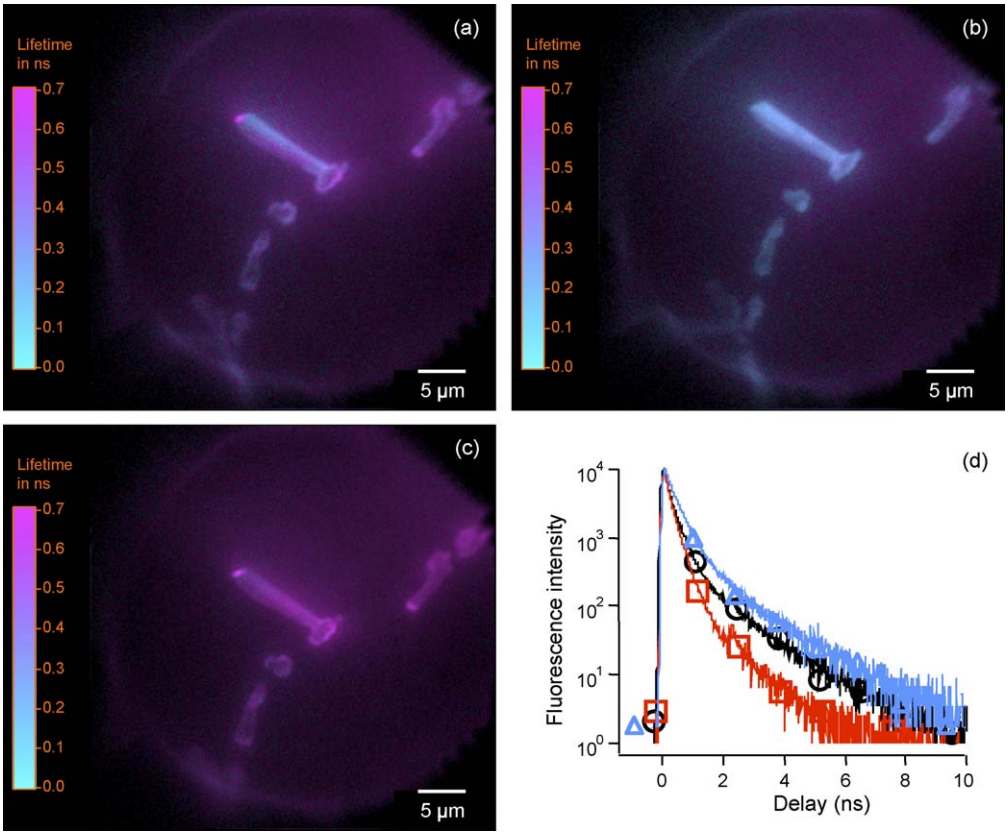

Fig. 5. FLIM images of casted films: (a) all-wavelength; (b) band-pass filter centered at 560 nm; (c) band-pass filter centered at 619 nm; (d) fluorescence intensity decays corresponding to: (●) image (a); (■) image (b); (▲) image (c). Image (b) corresponds to the fluorescence of the monomer and image (c) to the fluorescence of the excimer. The fluorescence of the monomer is quenched all over the film. The excimer concentration is not homogeneous over the film.

Finally, microcrystals obtained from a large amount of a concentrated solution of TMB in dichloromethane were observed. The fluorescence spectrum is shown in Fig. 4. The maximum of fluorescence is at 608 ± 3 nm. Because of the thickness of the sample, the absorption spectrum could not be recorded. The fluorescence decay is monoexponential with a lifetime of 9.5 ns. When these single crystals are smashed with a spatula, the fluorescence decay becomes multiexponential. Attempts to prepare MB single crystals have not been successful. In single microcrystals there is only one emitting excimer.

The QA is a powerful tool to image the distribution of monomers and excimers in each sample. QA FLIM and intensity images of TMB films are displayed in Fig. 5. Each picture displays intensities (associated with brightness on the pictures) and mean lifetime (colour) data. Fig. 5a contains information from all the emission wavelengths. Intensity and lifetime are not homogeneous all over the sample. Filters were used to study the fluorescence of the monomers and of the excimers. Fig. 5b was taken with a band-pass filter centred at 560 nm. It shows that the monomer fluorescence, measured at 560 nm, comes from all over the aggregates with a homogeneous intensity and a shorter lifetime compared to the total fluorescence, measured without filters. For Fig. 5c a band-pass filter centred at 619 nm was used. According to this picture, excimer emission has a longer lifetime and the intensity is higher in specific areas. Fig. 5d displays the fluorescence decays calculated on the biggest aggregate for each picture. The same evolution of the lifetime is observed. Similar experiments were performed on MB films with band-pass filters centred at 560, 639, and 741 nm. Without filters, the mean fluorescence lifetime is 1.30 ns. With filters lifetime of 1.07, 1.50 and 1.56 ns were observed. Gathered in Table 2 are the wavelengths, global lifetimes and lifetimes recorded at different wavelengths corresponding to these experiments. Fig. 6 shows a QA image of a 50 μm large single crystal. The fluorescence intensity and lifetime are homogeneous all over the crystal and the fluorescence decay is monoexponential with a lifetime of 9.5 ns.

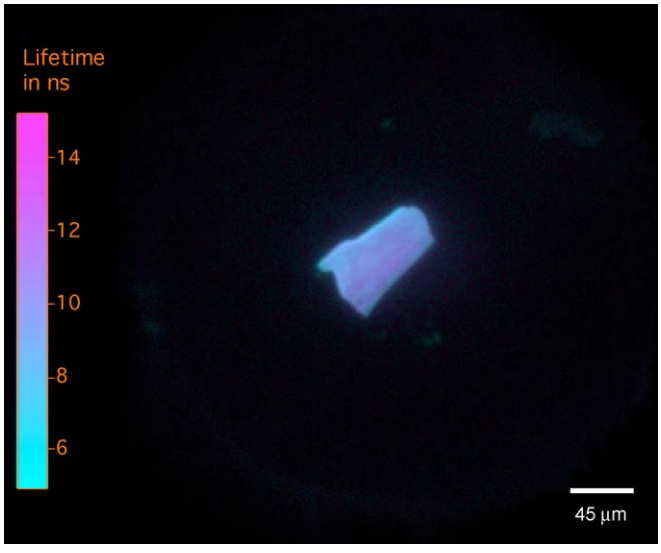

Fig. 6. FLIM image of a TMB single crystal. The fluorescence decay is homogeneous on the crystal and monoexponential with a lifetime of 9.5 ns.

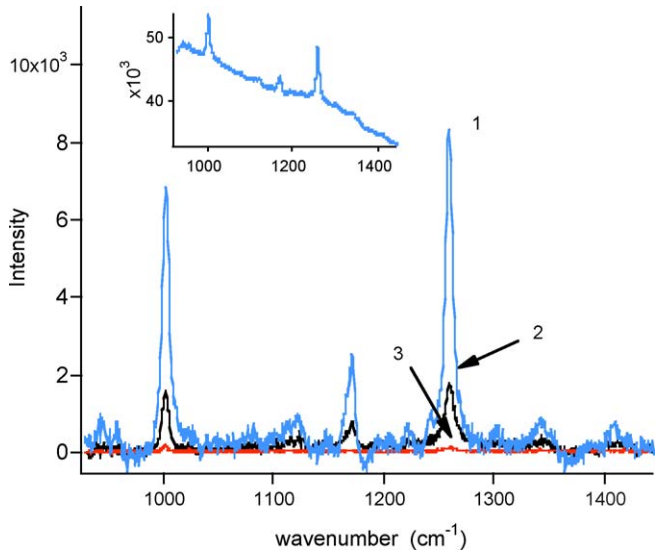

Fig. 7. Raman spectra of: (1) TMB single crystal, (2) and (3) TMB casted films. The signal corresponding to the fluorescence has been removed via a baseline subtraction. Molecules in a crystal state have narrow Raman bands. In amorphous areas the Raman bands are so broad that they cannot be seen over the fluorescence background. Inset: Raman spectra of the TMB single crystal before baseline subtraction.

In order to estimate the crystallinity of our samples, Raman spectroscopy was performed [39]. The spectra recorded for a single crystal and casted films are displayed in Fig. 7. The spectra are centred at $1200\,cm^{-1}$. Three maxima are observed at 1002, 1172 and $1259\,cm^{-1}$. An important background signal was observed on rough data, due to the fluorescence of the samples (see inset in Fig. 7). For clarity's sake, this signal was removed on the spectra displayed in Fig. 7 using a baseline subtraction method. For the single crystal, the peaks are sharp and intense, which is characteristic of the crystalline state. On the contrary, much weaker peaks are observed on the spectra of the casted films. When the degree of crystallinity of a solid decreases, the Raman bands get wider and the maximum of the peak decreases. According to these spectra, we can say that the casted films are mainly amorphous.

The formation of two ground state excimers (D_I and D_{II}) of Bodipy derivatives has been reported [40–42]. D_I is an H aggregate formed by stacking two Bodipy planes with parallel $S_0 \rightarrow S_1$ transition dipoles and anti-parallel electric dipole moments. In D_I, the absorbance spectrum is blue shifted and no fluorescence has been observed. D_{II} is a J aggregate where the bodipy molecules and the $S_0 \rightarrow S_1$ transition dipoles are oriented in a plane. It has a red-shifted absorption spectrum and is fluorescent. Energy transfer from a monomer in its excited state to an excimer (D_I or D_{II}) in its ground state has been observed [40]. The absorption of D_{II} presents a good spectral overlap with the fluorescence of the monomer that favours an energy transfer from the monomer to the excimer.

In TMB cast films, the absorption spectra show a monomer absorption peak broadened by strong intermolecular interactions. The fluorescence emission spectra show both monomer and excimer emission. According to the results displayed in

Table 3
Properties of the nanocrystals in sol–gel thin films

	d	Catalysis	Particle size (nm)	Lifetime (ns) [χ^2]
MB1	1×10^{-2}	Acid	650	1.27/0.30 [1.06]
MB2	1×10^{-3}	Acid	450	1.95/0.45 [1.05]
TMB1	5×10^{-3}	Acid	<500	3.65/1.44 [1.07]
TMB2	1×10^{-3}	Acid	400	5.49/2.24 [1.19]
TMB3	1×10^{-3}	Acid–base	100	5.24 [1.13]

Fig. 5, the monomer is present all over the solid whereas the excimer is localized at the periphery. The presence of non-fluorescent excimers can be deduced from the reduction of the fluorescence lifetime of the monomer, compared to the lifetime in dichloromethane. Since this lifetime is the same all over the solid, the quenching of the fluorescence of the monomer is uniform in the sample. As the fluorescence of the excimer varies in the sample, the fluorescence of the monomer is quenched by at least two different types of defects; non-fluorescent excimers in the core of the film and fluorescent ones at the periphery.

There is only one fluorescent species in TMB single crystals because the fluorescence spectrum has one maximum and the decay is monoexponential with a fluorescence lifetime of 9.5 ns. As the fluorescence is red-shifted by more than 50 nm compared to TMB in dichloromethane, this fluorescence can be attributed to an excimer. Even if no MB single crystals were studied, we can expect that a single fluorescence emission would not be observed, since no evolution is observed when going from film to powder.

In the crystalline state, formation of excimers is favoured whereas two fluorescent species coexist in the non-crystalline state. The fact that the fluorescence decay becomes multiexponential when a single crystal is smashed shows that the fluorescence is quenched at structural defects.

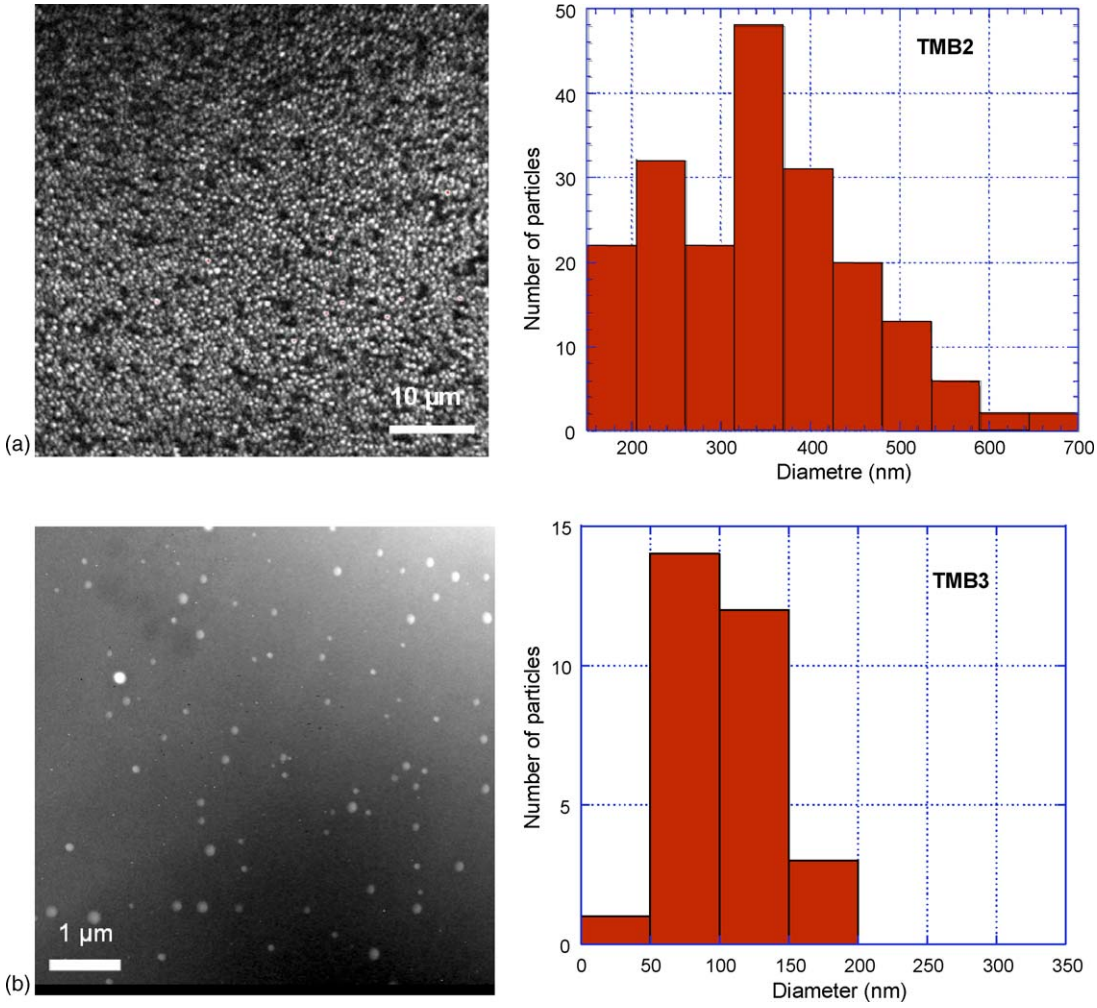

Fig. 8. (a) Confocal microscopy image of sample TMB1 and (b) transmission electron microscopy image of sample TMB3.

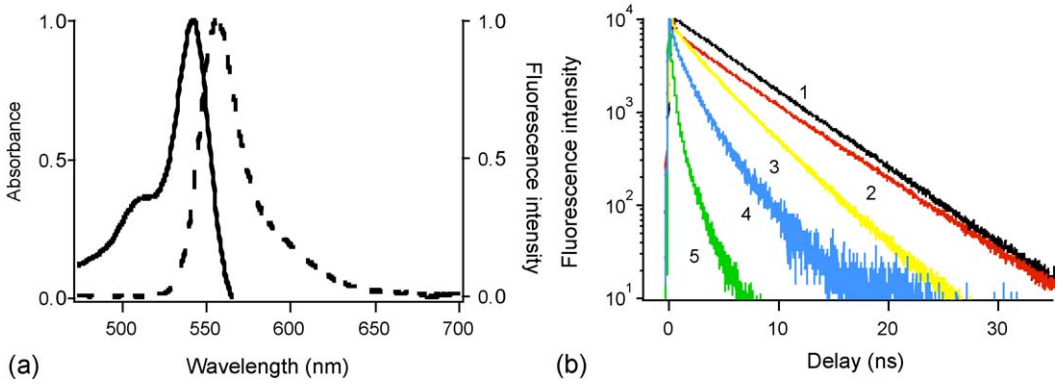

Fig. 9. (a) (—) Absorption and (— —) fluorescence spectra of TMB microcrystals in sol–gel thin films (sample TMB3). The shapes of the spectra are similar to the one of TMB dissolved in dichloromethane. (b) Fluorescence intensity decays of nanocrystals in sol–gel thin films: (1) TMB3; (2) TMB2; (3) TMB1; (4) MB2; (5) MB1. The decay curves are fitted by a double exponential, except for the decay of the smallest TMB crystals (TMB3) which is fitted by a single exponential function.

3.3. Nanocrystals in sol–gel thin films

In order to study the feasibility of a nanosensor with these Bodipy dyes, nanocrystals grown in sol–gel thin films were prepared. Two or three samples for each Bodipy were studied, MB1 and MB2 for MB and TMB1 to TMB3 for TMB. Table 3 shows results obtained for these samples. The structure of samples MB1 and MB2, TMB1 and TMB2 were studied by confocal microscopy and sample TMB3 by TEM (see Fig. 8). With mesitylbodipy (MB), crystals with a diameter between 200 and 650 nm were obtained. For sol–gel prepared with trimesitylbodipy (TMB), crystals have a large distribution of diameter with a maximum of 500 nm in sample TMB1 and a thinner distribution centred around 400 nm in sample TMB2. The nanocrystal density is very high in these samples. TEM microscopy of sample TMB3 shows particles with a mean diameter of 100 nm.

As shown in Table 2, nanocrystals in sample TMB3 are smaller than in the other samples. This is due to the sample preparation. Indeed, the sol–gel of samples MB1 to MB2, TMB1 and TMB2 were prepared with acid catalysis (one-step), whereas that of sample TMB3 was prepared with acid–base catalysis (two-step). The pH during sol formation controls the ratio between hydrolysis and condensation kinetics, which is a way of tuning the size of the reactor where nucleation of the crystals takes place. The nanocrystals formed in acid–base conditions are smaller because the nucleation and growth take place in smaller reactors [30,31].

Absorption and fluorescence spectra of sample TMB3 are shown in Fig. 9a. The spectra of nanocrystals are similar to those of TMB dissolved in dichloromethane. Fluorescence spectra are similar to those of the other samples, but a small broadening of the red edge of the absorption spectrum is observed when going from TMB3 to TMB1. Fluorescence decay of TMB in sol–gel thin-films are shown in Fig. 9b. For samples TMB1 and TMB2 the global decay is bi-exponential. The two components are roughly 3.5 and 1 ns for TMB1 and 5 and 1 ns for TMB2. The global fluorescence decay of sample TMB3 is a single exponential with a lifetime of 5.2 ns. Fig. 9b also displays the fluorescence decays of sample MB1 and MB2. Both decay can be fitted by a double exponential function, with lifetimes of 1.27 and 0.30 ns for sample MB 1 and 1.95 and 0.45 for sample MB2.

An increase in the mean fluorescence lifetime of nanocrystals grown in sol–gel thin films is seen going from MB to TMB: π-stacking is less probable in the case of TMB compared to MB, due to a better steric protection by the two added mesithyl groups. Thus, MB is more likely to form amorphous aggregates than TMB.

According to their fluorescence spectra, the three samples made with TMB exhibit a monomer-like fluorescence. For crystals bigger than 100 nm, time-resolved experiments show that the fluorescence is complex. This might be attributed to their degree of crystallinity, concentration of defects, or size. So far no conclusion can be made. Nevertheless in 100 nm crystals, fluorescence behaviour shows that only one species is present (single exponential decay). As the absorption and fluorescence maxima are close to those recorded in dichloromethane, it is a monomer-like fluorescence. Such nanoparticles could be used as sensors in the future. Indeed it has already been demonstrated that nanocrystals in sol–gel matrix, prepared with other fluorophores, have been used for sensing [15].

4. Conclusion

In this paper we have presented the fluorescence properties of two bodipy derivatives. The addition of bulky groups to the Bodipy chromophore has improved the fluorescence of this molecule in solution and in aggregates. Indeed, when we compare TMB and MB emission properties, the fluorescence quantum yield of the former is higher in dichloromethane. In crystalline state, the fluorescence lifetime also increases (either for nanocrystals embedded in a sol–gel matrix or for microcrystals). Moreover TMB monocrystals exhibit an excimer fluorescence with a lifetime of 9.5 ns. Such evolution is attributed to the two added mesityl groups that limit π-stacking and non-luminescent deactivation pathways.

Because it can form two fluorescent species in the solid state, TMB is not the best candidate to prepare luminescent nanocrystals. Nevertheless it is an interesting fluorophore. The two Bodipys presented here can be used to prepare fluorescent

latex beads [7]. In order to understand better the solid-state fluorescence of TMB, its crystalline structure will be studied by X-ray diffraction. Moreover the synthesis of Bodipys with more bulky substituents is under progress.

References

[1] O.S. Wolfbeis, in: B. Culshaw, J. Dakin (Eds.), Optical Fiber Sensors, vol. 4, Artech House, Boston-London, 1997, p. 53.
[2] B. Valeur, in: J.R. Lakowicz (Ed.), Topics in Fluorescence Spectroscopy, vol. 4, Plenum Press, New York, 1994, p. 21.
[3] M. Orrit, J. Bernard, Phys. Rev. Lett. 65 (1990) 2716–2719.
[4] S. Weiss, Science 283 (1999) 1676–1683.
[5] C. Saudan, V. Balzani, P. Ceroni, M. Gorka, M. Maestri, V. Vicinelli, F. Vögtle, Tetrahedron 59 (2003) 3845–3852.
[6] V. Balzani, P. Ceroni, S. Gestermann, M. Gorka, C. Kauffmann, F. Vögtle, Tetrahedron 58 (2002) 629–637.
[7] R. Méallet-Renault, R.B. Pansu, S. Amigoni-Gerbier, C. Larpent, Chem. Commun. 20 (2004) 2344–2345.
[8] T. Förster, Naturwiss (1946) 166–175.
[9] M. Pauchard, S. Huber, R. Méallet-Renault, H. Maas, R.B. Pansu, G. Calzaferri, Angew. Chem. Int. Ed. 40 (2001) 2839–2842.
[10] R. Métivier, T. Christ, F. Kulzer, T. Weil, K. Müllen, T. Basche, J. Luminesc. 110 (2004) 217–224.
[11] M. Lor, L. Viaene, R. Pilot, E. Fron, S. Jordens, G. Schweitzer, T. Weil, K. Mullen, J.W. Verhoeven, M. Van der Auweraer, F.C. De Schryver, J. Phys. Chem. B 108 (2004) 10721–10731.
[12] R. Méallet-Renault, P. Denjean, R.B. Pansu, Sens. Actuators B 59 (1999) 108–112.
[13] D. McQuade, A. Pullen, T. Swager, Chem. Rev. 100 (2000) 2537–2574.
[14] J.P. Desvergne, T. Brotin, D. Meerschaut, G. Clavier, F. Placin, J.L. Pozzo, H. Bouas-Laurent, New J. Chem. 28 (2004) 234–243.
[15] F. Treussard, E. Botzung-Appert, N.T. Ha-Duong, A. Ibanez, J.F. Roch, R.B. Pansu, ChemPhysChem 4 (2003) 757–760.
[16] Z. Huang, E. Terpetschnig, W. You, R. Haugland, Anal. Biochem. 207 (1992) 32.
[17] F. Bertorelle, D. Lavabre, S. Fery-Forgues, J. Am. Chem. Soc. 125 (2003) 6244–6253.
[18] J.H. Boyer, A.M. Haag, G. Sathyamoorthi, M.L. Soong, K. Thangaraj, T.G. Pavlopoulos, Heteroatom. Chem. 4 (1993) 39–49.
[19] A. Costela, I. Garcia-Moreno, C. Gomez, R. Sastre, F. Amat-Guerri, M. Liras, F.L. Arbeloa, J.B. Prieto, I.L. Arbeloa, J. Phys. Chem. A 106 (2002) 7736–7742.
[20] K. Yamada, T. Toyota, K. Takakura, M. Ishimaru, T. Sugawara, New J. Chem. 25 (2001) 667–669.
[21] T. Kalai, E. Hideg, J. Jeko, K. Hideg, Tetrahedron Lett. 44 (2003) 8497–8499.
[22] K. Rurack, M. Kollmannsberger, U. Resh-Genger, J. Daub, J. Am. Chem. Soc. 122 (2000) 968–969.
[23] A. Coskun, E.U. Akkaya, J. Am. Chem. Soc. 127 (2005) 10464–10465.
[24] (a) H.C. Kang, R.P. Haugland, Ethenyl-Substituted Dipyrromethene boron Difluoride Dyes and Their Synthesis, Molecular Probes, Inc., Eugene, Oregon, USA, 1993;
(b) H.C. Kang, R.P. Haugland, Dibenzopyrromethene boron Difluoride Dyes, Molecular Probes, Inc., Eugene, Oregon, USA, 1995.
[25] H. Langhals, R. Ismael, O. Yürük, Tetrahedron 56 (2000) 5435–5441.
[26] S. Yokohama, A. Otomo, T. Nakahama, S. Mashiko, Thin Solid Films 393 (2001) 124–128.
[27] A.B. Zaitsev, R. Meallet-Renault, E.Y. Schmidt, A.I. Mikhaleva, S. Badre, C. Dumas, A.M. Vasil'tsov, N.V. Zorina, R.B. Pansu, Tetrahedron 61 (2005) 2683–2688.
[28] M. Kollmansberger, K. Rurack, U. Resh-Genger, J. Daub, J. Phys. Chem. A 102 (1998) 10211–10220.
[29] J. Zaccaro, et al., C. R. Phys. 3 (2002) 463–478.
[30] A.H. Boonstra, T.M.N. Bernards, J. Non-Cryst. Solids 105 (1988) 207–213.
[31] C. McDonagh, P. Bowe, K. Mongey, B.D. McGraith, J. Non-Cryst. Solids 306 (2002) 138–148.
[32] N. Sanz, A.C. Gaillot, P.L. Baldeck, A. Ibanez, J. Mater. Chem. 10 (2000) 2723–2726.
[33] L. Schoutteten, P. Denjean, R.B. Pansu, J. Fluoresc. 7 (1997) 155–165.
[34] K.A. Levenberg, Appl. Math. II 2 (1944) 164.
[35] M. vdVen, M. Ameloot, B. Valeur, N. Boens, J. Fluoresc. 15 (2005) 377–413.
[36] G. Ullrich, R. Ziessel, J. Org. Chem. 69 (2004) 2070–2083.
[37] A. Burghart, H. Kim, M.B. Welch, L.H. Thoresen, J. Reibenspies, K. Burgess, F. Bergstro, L.B. Johansson, J. Org. Chem. 64 (1999) 7813–7819.
[38] H. Kim, A. Burghart, M.B. Welch, J. Reibenspies, K. Burgess, Chem. Commun. (1999) 1889–1890.
[39] G. Herzberg, Infrared and Raman Spectra of Polyatomic Molecules, vol. 2, D. Van Nostrand Company, New York, 1950.
[40] F. Bergstrom, I. Mikhalyov, P. Hagglof, R. Wortmann, T. Ny, L.B.A. Johansson, J. Am. Chem. Soc. 124 (2002) 196–204.
[41] I. Mikhalyov, N. Gretskaya, F. Bergstrom, L.B.A. Johansson, Phys. Chem. Chem. Phys. 4 (2002) 5663–5670.
[42] D. Tleugabulova, Z. Zhang, J.D. Brennan, J. Phys. Chem. B 106 (2002) 13133–13138.